ACTA STEREOL 1999; 18/3: 415-425
ORIGINAL SCIENTIFIC PAPER

AUTOMATIC SEGMENTATION FOR DNA PLOIDY MEASUREMENTS: METHODOLOGICAL CHOICES

Belhomme P.[1], Herlin P.[2], Elmoataz A.[3], Rougereau O.[4], Boudry C.[2], Bloyet D.[3]

[1]LUSAC - EIC, Site Universitaire de Cherbourg, B.P. 78, 50130 Octeville, France
[2]Lab. d'Anatomie-Pathologie, Centre F. Baclesse, Route de Lion/mer, 14021 Caen, France
[3]GREYC - CNRS, UPRESA 6072, 6 Boulevard Maréchal Juin, 14050 Caen, France
[1,2,3,4]Pôle Traitement et Analyse d'Images de Basse-Normandie (*TAI*)

ABSTRACT

Image cytometry (ICM) makes it possible to measure DNA content of cancer cell nuclei in a fully automatic and reproducible way. DNA ICM relies on a three step procedure : segmentation of all the nuclei collected in a series of images, followed by computation of integrated optical density (IOD) of DNA specific stain and morphometric parameters, then on elimination of unwanted elements, thanks to a selective sorting of parameters. Quality of sorting is closely linked to the accuracy of the computed parameters, these later depending of course on the quality of segmentation. The present paper studies the impact of the segmentation step on the number of nuclei to be measured, on their size and their IOD. The study reveals that the choice of one segmentation method over another may involve a great disparity in measurements, e.g. in the percentage of aneuploid cells and in the size of the proliferating cell compartment.

INTRODUCTION

To the pathologist the estimation of nuclear DNA content offers a tool for evaluating the potential aggressiveness of tumors. This measurement can be based on image analysis which represents, thanks to its possibilities of cell sorting, an attractive alternative to the more widely used flow cytometry (FCM) (Marchevsky et al., 1994). We underlined that ICM is best suitable to clinical practice. This automation should lead to precise and reproducible measurement of IOD of the DNA stained nuclei, and reliable sorting out of unwanted elements (debris, aggregates, normal inflammatory and stromal cell nuclei). The recent ESACP consensus report has reviewed the main causes of error in DNA ICM, but the potential errors caused by a bad segmentation have only been briefly mentioned (Böcking et al., 1995). However, the quality of the segmentation process has probably a significant impact on IOD computation as well as on computation of the morphological parameters used for automated cell sorting. To the best of our knowledge, no work has been published on this subject. The objective of the present study is thus to evaluate the repercussion of the segmentation step, by testing some procedures belonging to the main families of algorithms, and to provide a methodology for choosing the best one for the goals of the analysis.

MATERIALS

The acquisition system is based on an Olympus BH2 microscope coupled to a mono CCD camera (Sony) connected to a PC running under UNIX operating system. The PC includes a black and white frame grabber (Matrox PIP 1024) delivering images of size 512x512 in 256 gray levels. With an objective X20 (numerical aperture 0,70) and a X6.25 projective unit (leading to a final magnification X 125), each pixel in an image corresponds to a surface of 0.11 μm^2. For the present study, a series of 388 images of dissociated cell nuclei, stained according to Feulgen and Rossenbeck method (Feulgen et al., 1924), has been acquired and backed up on hard disc. This series is made up of 193 images acquired from normal breast tissue and 195 images acquired from a case of high grade breast cancer. In the following parts of this paper these two series will be respectively designed as "sample 0" and "sample 1". A manual counting has revealed the presence of 6418 objects belonging to all the categories of intact nuclei and aggregates and debris.

The image processing system is structured around a IBM RISC 6000/AIX workstation. DRACCAR© software, developed in our laboratory (Masson et al., 1992), allows to segment the images to isolate the relevant objects, then to measure, sort and analyze them, in order to build a DNA ploidy histogram from which the unwanted cellular categories can be removed (nuclei of inflammatory and stromal cells, debris, aggregates...).

METHODS

A. Generalities and Principles

There is no universal technique of segmentation up to now but in fact several operators and methods which are traditionally classified in four families :

F1 : methods based on grey level histogram analysis (thresholding)
F2 : methods based on object contour detection
F3 : methods based on region growing
F4 : hybrid methods combining operators of the three first families.

The use of operators from only one family is generally sufficient on simple images (with limited information) but in the biomedical field, where images are generally more complex, it is more often necessary to chain operators belonging to several families, in order to reach an acceptable segmentation quality. The choice of methods must be both guided by an accurate analysis of image characteristics and by degree of precision needed (object counting for example will require a lower degree of accuracy than surface measurement). We will briefly review the principles and properties of the four families of methods.

F1 : methods based on grey level histogram analysis (thresholding)

When a class of objects is characterized by a specific distribution of grey levels, it may be highlighted through application of characteristic thresholds. Automatic detection can then apply several methods (Sahoo et al., 1988). The operators of this family have the advantages of running fast and being easy to implement, but they are not stable enough from one image to another.

F2 : methods based on object contour detection

The contour-based methods rely on the detection and localization of object borders by means of more or less elaborated differential operators, which are associated to a regularization

process (required by the discretization of images). Unfortunately, these methods often lead to unclosed contours when they are applied to strongly textured objects or slightly contrasted images.

F3 : methods based on region growing

These methods try to isolate some regions respecting one or more homogeneity criteria. Regions are extracted either by successive fusion of the original image until they all respect the defined criteria (ascending analysis) or by progressive growing of connected pixels while the criteria are observed (descending analysis). In the last case, the region growing process can be iterated from single points (designed as « seeds ») or from greater areas provided by another segmentation step.

F4 : hybrid methods combining operators of the three first families

These segmentation methods combine both « contour » and « region » features in the same process. One may mention the watershed algorithm in mathematical morphology (Beucher, 1992) or the active contour methods (Kass et al., 1988). The residual analysis is a particular technique which can be included in this family. It consists in processing two smoothings of an image (a strong one and a weak one) then to calculate the difference between the two results. This operation is quite similar to the computation of a Laplacien filter (differential operator). By thresholding only the positive values of the result one then forms some homogeneous regions.

B. Segmentation methods tested

Nine segmentation methods covering the four families above-mentioned have been tested in this study (cf. Table 1 for details). Method 0 belongs to the contour-based family (F2). Methods 1 and 2 combine a residual analysis (F4) and a thresholding (F1). Methods 3 to 6 are hybrid techniques (F4) making use of region growing (F3) and thresholding (F1) procedures while methods 7 and 8 are only related to histogram analysis (F1).

M0 : This is the method implemented in DRACCAR© software. It relies on the Canny-Deriche contour detection operator (Deriche, 1987) which includes a regularization step based on recursive exponential filtering. Once the main contours are extracted (those having the greatest values in the image of frontiers), a frontier closing automaton is applied to form the objects.

M1 : This method consists in finding the minimum between two images, one provided by the thresholding technique of interclass variance maximization (IVM), and one provided by a residual analysis.

M2 : This method consists in finding the minimum between two images, one provided by the thresholding technique of entropy minimization (EM), and one provided by a residual analysis.

M3 : This method first consists in applying a IVM thresholding in order to extract the background region. The first pixel of the background (starting in the upper left corner) stands for the seed from which a region growing process is realized. The homogeneity criterion used to control the growing process is that the absolute difference between the grey level value of a pixel and the mean grey level value of the adjacent region has to be lower than 40.

M4 : Same method than the previous one but with EM thresholding.

M5 : This method first consists in applying a IVM thresholding in order to extract the background region. The same steps as in the T3 technique are then applied but the growing process is directly conducted from the background region (and not from a single point).

Table 1 : General principles of the nine tested segmentation methods (a "X" indicates the type of performed operations).

	General principles of methods		Method number								
			0	1	2	3	4	5	6	7	8
F1	Histogram	Variance		X		X		X		X	
		Entropy			X		X		X		X
F2	Contour	Canny-Deriche	X								
F3	Region growing	Seed = 1 point				X	X				
		Seed = background						X	X		
F4	Hybrid	Residual analysis		X	X						

M6 : Same method as the previous one but with EM thresholding.

M7 : This method consists in a classic IVM thresholding followed by very simple cleaning procedures by means of morphological openings (size 2).

M8 : Same method as the previous one but with EM thresholding.

C. Methodology of comparison

All the objects lying on the 388 images have been manually checked in Corel Photopaint 6© by writing on the overlay. This action provides the first series of binary images standing for the reference. A specific software, developed in C for UNIX operating system, has been used to compare the results of all the segmentation methods (expressed as a second series of binary images) to the manual counting. This software allows to create, for each segmentation method, a third series of binary images containing only the common objects. It then computes, by comparing the three series, the number of omitted objects and the number of false objects. The aggregates covering several manual checks are counted only once.

In a first time, the numerical evaluation has been conducted on the primary population, that means without any sorting of unwanted cells such as stromal or inflammatory cells and without elimination of debris and aggregates. Object counting has been achieved on the 388 images. The best fitted automated method will present the higher percentage of common objects and the lower percentages of false and omitted objects. Quality segmentation in term of object number may be estimated thanks to the following criterion :

$$Q_s = |\ 100\% - \%\ \text{Common obj.}\ | + \%\ \text{Omitted obj.} + \%\ \text{False obj.}$$

On the primary population, the surface modal value as well as the surface minimum and maximum values have been estimated too. The observed variations, for any value V, are expressed as a relative difference according to the formula:

$$D_r = \frac{V_{\max} - V_{\min}}{V_{\min}}$$

The mean and standard deviation (SD) of DNA content, as well as the mode of the diploid peak of the reference sample (sample 0) and the mode of the aneuploid peak of the cancer sample (sample 1) have been computed. The percentage of hypoploid elements (those with a DNA content located before the diploid peak, normally corresponding to small nuclear debris) as well as the percentage of cells having a DNA content higher than 5c are retained as

parameters allowing to estimate the segmentation quality. The observed variations are also expressed in the form of relative differences.

Automatic classification of segmented elements has been completed by DRACCAR© software by means of a multi-parametric analysis (with 38 parameters) and by reference to a learning base (Herlin et al., 1997). All the evaluations presented below are only related to the epithelial compartment. Quality of any segmentation method may then be estimated by comparing the automatic object sorting to a visual sorting by an expert. A numerical parameter Q_t, expressing the segmentation quality before automatic sorting, can be computed according to the following formula:

$$Q_t = \left| Nb\ EC_{auto} - Nb\ EC_{man\ ref} \right|$$

with $Nb\ Ec_{auto}$ = number of epithelial cells automatically found
$Nb\ Ec_{man\ ref}$ = number of epithelial cells of the manual reference

The best segmentation method should give the lowest Q_t.

DNA ploidy measurement accuracy can be estimated by computing the coefficient of variation (CV) of the G0-G1 diploid peak (sample 0) and the aneuploid peak (sample 1). This has been realized thanks to the DNA data analyzer software McycleAv© (Phoenix Flow System). A good segmentation method must generate thin peaks (so with low CV).

Finally, the percentage of aneuploid cells in the tumor (percentage of cells in the G0-G1 aneuploid peak and percentage of cells in the aneuploid cycle) and the proliferating compartment (percentage of cells located after the aneuploid peak) have been computed by a specific data processing software embedded in DRACCAR©. This software makes Gaussian fits (no more than 3) in order to find on the ploidy histogram the G0-G1 population, then tries to estimate the number of elements located after the raw aneuploid peak and after the corrected aneuploid peak (correction yielding to count for 100% the aneuploid cycle). Relative differences for all these parameters are also indicated. The last parameter extracted from the ploidy histogram is the Auer typing which offers the advantage of being a combination of DNA aneuploid measurements and proliferation measurements.

RESULTS

Analysis of raw data : object counting

The number of found objects, common objects, omitted objects as well as the number of false objects returned by the nine segmentation methods (by reference to the manual check of 6418 elements) are presented in the Table 2 and visualized on the histogram of Figure 1.

Table 2 : Object counting

Tech.	Found objects	Common objects	Omitted objects	False objects
0	80.71%	74.81%	25.19%	5.91%
1	84.82%	82.42%	17.84%	2.40%
2	94.16%	85.95%	13.70%	8.21%
3	87.25%	81.61%	18.00%	5.64%
4	87.10%	83.03%	16.13%	4.07%
5	85.31%	82.67%	17.47%	2.63%
6	85.35%	82.69%	17.45%	2.66%
7	123.84%	84.59%	16.92%	39.25%
8	272.41%	87.99%	11.05%	184.42%

Table 3 : Segmentation quality

Tech.	Q_s
2	35,96%
4	37,16%
5	37,43%
6	37,43%
1	37,82%
3	42,02%
0	56,29%
7	71,58%
8	207,48%

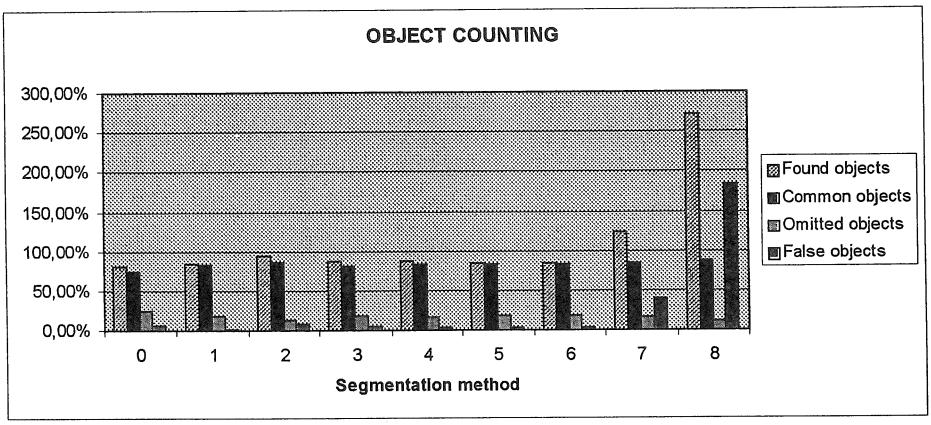

Figure 1 : Graphical representation of the object counting. The 100% line is the manual reference.

In the context of this study, the best segmentation method (lowest Q_s) is method number 2 which corresponds to a residual analysis combined with thresholding by entropy minimization (see Table 3 for methods sorted according to Q_s). However, the performances of techniques 1 to 6 are very close.

Analysis of raw data : object surface

The modal value as well as the minimum and maximum values of segmented object surface (expressed in pixels) are presented on Table 4 for two samples. The significant relative differences are computed.

Table 4 : Analysis of object surface provided by the nine segmentation methods.

		Segmentation methods									D_r max
		0	1	2	3	4	5	6	7	8	
S0	Mode	484	567	542	545	545	550	515	550	89	537%
	Min	42	26	26	39	39	34	34	34	45	
	Max	2105	2576	2582	3893	3893	3435	3435	3435	4460	111%
S1	Mode	142	216	216	174	193	146	146	129	220	70%
	Min	47	43	43	44	97	49	49	64	55	
	Max	2361	4327	4327	4361	9668	4860	4860	6446	5511	309%

There are large relative differences (D_r) for the modal surface values, ranging from 537% (sample 0) to 70% (sample 1). By removing the two segmentation methods based on classical thresholding (techniques 7 and 8) and showing the greatest variation, the relative differences fall to 17% and 52%, respectively. Differences observed for the minimum and maximum surface values are statistically significant for the last one; they reach 111% and 309%.

Analysis of raw data : DNA content abnormalities

Table 5 presents some measurements extracted from the ploidy histogram. It contains the mean and standard deviation (SD) of the DNA content distribution, the two modes of the sample 0 DNA diploid peak and sample 1 DNA aneuploid peak, the percentage of hypoploid elements and the percentage of objects whose DNA content is higher than 5c.

Table 5 : Analysis of object DNA content provided by the nine segmentation methods.

		Segmentation methods									D_r max
		0	1	2	3	4	5	6	7	8	
S0	Mean	1.58	1.65	1.64	1.71	1.72	1.73	1.73	1.74	1.55	12%
	SD	0.7	0.81	0.82	0.82	0.81	0.77	0.77	0.77	0.95	35%
	Mode	1.9	1.9	1.9	1.9	1.9	1.9	1.9	1.9	1.9	
	% hypo	32.8	29.4	30.1	27.6	27	24.9	24.9	25	35.2	41%
	% > 5c	0.09	0.32	0.31	0.35	0.34	0.32	0.32	0.32	0.39	333%
S1	Mean	1.72	1.91	1.84	1.90	1.96	2.04	2.04	2.02	1.78	18%
	SD	1.24	1.57	1.57	1.54	1.73	1.56	1.56	1.62	1.53	39%
	Mode	3	3	3	3	3	3	3	3	3.1	
	% hypo	22.4	22.7	23.4	21.7	20.8	17.4	17.2	19	23.7	37%
	% > 5c	1.86	3.11	3.08	3.43	3.59	3.81	3.78	3.59	2.92	104%

It may be observed that there are some variations for all the presented parameters except for modal values of diploid and aneuploid peaks which remain constant. Relative differences of mean DNA content are important since they get to 12% and 18% for the two samples. One may also observe that the two automatic thresholding techniques yield to extreme values, whereas these values remain stable inside a same family of methods (see for example results of method 1 and 2).

The relative differences of the standard deviation are twice more important since they reach respectively 35% and 39%.

The main disparities apply to percentages of DNA hypoploid elements (41% and 37%) and percentages of objects whose DNA content is higher than 5c (333% and 104%). The lowest results concerning objects beyond 5c are encountered with method 0 which is based on contour detection and closing.

Analysis of sorted populations : compartment of epithelial cells

DRACCAR© software allows classification of segmented objects in several categories by reference to its learning base. Epithelial cells of normal tissue are then distinguished according to their size or texture. Epithelial cells with abnormal morphology in tumor tissue are also discriminated from their size aberration, texture aberration or both of them. The other sorting categories cover stromal cells, lymphocytes, plasmocytes, unidentified non epithelial cells and debris. These last categories have to be removed before displaying the final ploidy histogram.

Table 6 presents the number of epithelial elements automatically found. The last column corresponds to a manual sorting conducted by an expert on the objects provided by segmentation method 0 ; it stands for the current reference.

Table 6 : Sorting of epithelial cells in the two samples.

		Segmentation method									
		0	1	2	3	4	5	6	7	8	man.
S0	Number of epithelial cells	1071	1085	1089	1082	1102	829	836	794	636	1018
	Total number of elements	2276	2529	2552	2290	2319	2184	2184	2196	2532	2276
	% epithelial cells	47%	43%	43%	47%	47%	38%	38%	36%	25%	44%
	Q_{t0}	**53**	**67**	**71**	**64**	**84**	**189**	**182**	**224**	**382**	
S1	Number of epithelial cells	851	955	959	804	870	686	689	553	801	735
	Total number of elements	2744	3311	3444	2977	3008	2914	2910	2866	3114	2744
	% epithelial cells	31%	29%	28%	27%	29%	24%	24%	19%	26%	27%
	Q_{t1}	**116**	**220**	**224**	**69**	**135**	**49**	**46**	**182**	**66**	
Q_t	$Q_{t0}+Q_{t1}$	**169**	**287**	**295**	**133**	**219**	**238**	**228**	**406**	**448**	

One can observe from Table 6 that percentages of recognized epithelial cells are not the same for all segmentation methods, the range spanning 22% of the scale in the two samples. Quality factor Q_t is very large for the thresholding techniques (n°7 and 8). Surprisingly, the minimal value of Q_t is encountered with method n°3 and not n°0 whereas the learning base is constructed from results provided by this last method.

Analysis of sorted populations : CV of diploid and aneuploid peaks

Table 7 presents the CV of the diploid and aneuploid peaks evaluated in McycleAv© (respectively in samples 0 and 1). The mean is indicated on the last line. The smaller mean value indicates more accurate measurement of DNA content. Except for method 0 which generates a great CV, all the others provide close results.

Analysis of sorted populations : DNA content abnormalities in sample 1

We are only interested here by DNA content anomalies (sample 1). The measured parameters are presented in Table 8. One can observe some large relative differences in these results, especially for percentages of cells located after the aneuploid peak (with or without correction). A direct effect is that method 2 generates a different Auer typing than all the other methods. Indeed, the Auer typing is deduced from the third parameter by testing if it is lower than 5% or not.

Table 7 : Coefficients of variation (CV) of diploid and aneuploid peaks.

	Segmentation method								
	0	1	2	3	4	5	6	7	8
CV of G0-G1 diploid peak	4.2	3.2	3.2	3.3	3.3	3.4	3.5	3.2	3.1
CV of G1 aneuploid peak	4.0	3.6	3.8	3.6	3.6	3.8	3.9	3.9	3.7
Mean CV	4.1	3.4	3.5	3.45	3.45	3.6	3.7	3.55	3.4

Table 8 : DNA content anomalies of epithelial cells (sample 1).

	Segmentation methods									D_r
	0	1	2	3	4	5	6	7	8	
% in aneuploid peak	65,8	66,0	76,0	58,9	62,5	70,2	70,4	74,0	62,6	29%
% > aneuploid peak	7,7	6,8	3,8	5,6	6,0	6,9	6,9	10,0	5,1	163%
% > corrected aneuploid peak	10,5	9,4	4,8	8,7	8,7	8,9	8,9	11,9	7,5	148%
% in aneuploid cycle	73,5	72,8	79,8	64,5	68,5	77,1	77,3	84,0	67,7	30%
Auer typing	IV	IV	III A	IV	IV	IV	IV	IV	IV	

DISCUSSION

In order to synthesize the presented results, one can say that considerable differences are observed, according to the segmentation method used, on three types of parameters computed on objects : number, surface and DNA content. In fact, the final measure we are interested in is the DNA ploidy histogram which relies on a good quality of cell sorting in order to dismiss unwanted elements. But the three types of parameters all have an impact more or less significant on both ploidy histogram and sorting results.

For example, the number of segmented objects essentially influences the shape of DNA ploidy histogram. So, the loss of biggest elements decreases the detection sensitivity of rare elements, those which are the more pertinent since they sign a starting aneuploidy or proliferation. On the other hand, the gain of small objects inflates the left part of ploidy histogram and also yields to decreasing the detection sensitivity. The gain of objects, whatever their size, has also an impact on sorting by involving a larger useless time processing.

Surface estimation accuracy influences IOD measurements and, by the way, location of segmented objects in DNA ploidy histogram. Indeed, IOD is obtained from the following formula :

$$IOD = \sum_{(x,y)\in nucleus} Log_{10}\left(\frac{I_i(x,y)}{I_t(x,y)}\right)$$

$I_i(x,y)$: incident light in (x,y)

$I_t(x,y)$: transmitted light in (x,y),

the ratio $\frac{I_i(x,y)}{I_t(x,y)}$ being equal to 1 for points belonging to the background, thus having a null logarithm value. Consequently, an object segmented outside its true limits will have its IOD nearly unchanged, whereas the same object segmented inside its limits will have its IOD largely decreased. Above all, surface estimation accuracy influences the sorting process since, among the 38 computed parameters, surface appears as one of the most discriminating parameter.

At last, accuracy of DNA content measurement, characterized by low CV of diploid and aneuploid peaks, determines the ability to discriminate near DNA diploid populations (those which are close to 2c value).

Considering all these remarks, a determined segmentation method can be chosen after analyzing its performances. The results provided by the nine tested segmentation methods are discussed below.

The contour-based method (n°0) generates the most reliable frontiers but is unable to extract all the objects (mainly the biggest ones) due to the relative complexity to efficiently tune the contour closing automaton. A bias is then produced on DNA ploidy histogram. In fact, this method produces the smallest number of objects (Table 2).

The two classic thresholding methods (n°7 and 8) produce the greatest number of objects, but many of them are false objects (Table 2). These false objects have then to be

distinguished from others by specific sorting algorithms that are never easy to tune. Our study reveals that two thresholding methods (variance and entropy) render different results (for object counting as well as DNA content). This is mainly due to the fact that methods based on histogram analysis do not give any control about frontier localization.

Methods making use of region growing processes, either from seeds or from areas (methods 3 to 6), are inclined to return object frontiers outside the true limits, thus leading to an overestimate of object surface. This has a direct impact on the later sorting. However, these 4 methods provide homogeneous and good results (a correct object counting without generating too many false objects).

Close to methods 3 to 6, methods 1 and 2 show the same properties but provide better results concerning object counting. Among them, method 2 (minimum between EM thresholding and residual analysis) appears as the best choice for our images thanks to its low Q_s parameter (cf. Table 2). This method combines EM thresholding with contour information via the residual analysis. This contour information explains the good results.

Methods 7 and 8, based on classic thresholding, provide the poorest results in nearly all domains and should be avoided for this type of image.

It may be noted that no manual reference is available concerning DNA content estimation. Indeed, a reference should be obtained from interactive outlining of nuclei but this would not be reliable enough (lack of precision and too much subjectivity). By analyzing DNA ploidy histograms through parameters of DNA aneuploid cycle one can note differences from a segmentation method to another. The only reliable indication on segmentation quality is the CV of peaks computed from standard populations.

Moreover, the presented results are strictly reliable only for the raw population, before sorting of cellular categories, since the sorting process used in this paper relies on a learning base constructed from results of method 0 (this last method being implemented in DRACCAR©). Nevertheless, it should be observed that when input values are changed, the automatic sorting process provides very different results (Table 6).

CONCLUSION

This study has shown that in the framework of image cytometry, choosing one automatic segmentation method rather than another yields to great disparities in the object number, and in measurements of object surface or DNA content. These disparities then cause variations in automatic cellular classification and in interpreting aneuploid cycle of epithelial cells from the DNA ploidy histogram. Our study reveals that analysis of cytological images, at first sight quite simple, needs sophisticated segmentation methods combining properties of several families of operators. Indeed, using operators from only one family (methods 0, 7 and 8) provide poor results which still can be largely improved. On the other hand, one has to note that our study is not exhaustive and many other attractive methods can be tested (for example watershed, active contours...).

Finally, we suggest that the method adapted for interpreting images should be tested on a standard population. Once a method is chosen and validated, a learning base must be created from its resulting segmented objects.

REFERENCES

Beucher S. The watershed transformation applied to image segmentation. *Scanning Microscopy*, sup. 6, p. 299-314, 1992

Böcking A, Giroud F, Reith A. Consensus of the ESACP task force on standardization of diagnostic DNA image cytometry. *Ann Cell Pathol*, 8, p. 67-74, 1995

Deriche R. Using Canny's criteria to derive a recursively implemented optimal edge detector. *Int Journal of Computer Vision*, 1, p. 167-87, 1987

Feulgen R, Rossenbeck H. Mikroskopisch-chemischer Nachweis einer Nukleinsäure vom typus der Thymonukleinsäure und die darauf beruhende elektive Färbung von Zellkernen in mikroskopischen Präparaten. *Hoppe Seyler's Z Physiol Chem*, 135, p. 203-24, 1924

Herlin P, Masson E, Duigou F, Plancoulaine B, Signolle JP, Mandard AM, Angot F, Deman D, Belhomme P, Joret JB, Datry T, Rougereau O, Bloyet D. Automatisation de l'analyse cytodensitométrique du contenu en ADN des tumeurs solides. *Bull Cancer*, 84(7), p. 685-92, 1997

Kass M, Witkin A, Terzopoulos D. Snakes: active contour models. *Int Journal of Computer Vision*, 1, p. 312-31, 1988

Marchevsky AM, Bartels PH. *Image analysis, a primer for pathologists.* Raven Press New York, 1994

Masson E, Herlin P, Bloyet D, Duigou F, Mandard AM. Image analysis optimization for the routine retrospective measurement of DNA ploidy of solid tumors. Part I. *Acta Stereol*, 11, p. 405-10, 1992

Sahoo PK, Soltani S, Wong AKC, Chen YC. A survey of thresholding techniques. *Computer Vision, Graphics, and Image Processing*, 41, p. 233-60, 1988

Presented at the 7th European Congress for Stereology, Amsterdam, April 20th to 23rd, 1998.